

AN AMBISONICS FORMAT FOR FLEXIBLE PLAYBACK LAYOUTS

Hannes Pomberger, Franz Zotter

IEM, University of Music and Performing Arts Graz, Austria (pomberger@iem.at, zotter@iem.at)

Abstract: *Ambisonics represents the sound field as a sum of angular modes (circular/spherical harmonics). The Ambisonics signals representing these angular modes are usually decoded to a set of loudspeakers by mode-matching equations. This works if the speakers are well-distributed on a circle or sphere. But Ambisonics playback arrangements frequently do not cover an entire circle or sphere due to practical constraints, which leads to non-trivial problems in decoder design. This paper presents two approaches to extend the capacities of Ambisonics to partial circular or spherical layouts by enabling decoder-design with mode-matching. The first approach selects suitable sets of harmonics, based on their symmetry and periodicity, and works for some particular partial layouts. But these selections are difficult to use for playback on default loudspeaker layouts, i.e. a full circle/sphere, and are not applicable to arbitrary partial layouts. So finally, the paper presents a second approach, which provides full flexibility of partial layouts, while enabling playback on full default layouts. This favored second approach is driven by a reduced set of signals, which can be utilized to optimize the requirements for storage and transmission. The authors propose to store and transmit the reduced set of signals within a file exchange format that includes an appropriate reconstruction matrix.*

Key words: Ambisonics, playback on partial domains.

1 INTRODUCTION

Ambisonics is a representation of the incident sound field on a spherical/cylindrical surface based on an expansion into a number of circular/spherical harmonics signals [1, 2], the *Ambisonics signals*. Using a finite order of harmonics signals results in an ideally smooth limited angular resolution for all angles of incidence on the surface of reproduction. Ambisonics is a viable down-mix format for spatialization of many virtual sources, since its reproduction including dynamic binaural rendering is well-proven and computationally inexpensive. Ambisonics signals are also suitable for recording the incident sound field at the surface of a spherical microphone arrays [3, 4, 5]. Furthermore, it is suitable for the representation of the radiation from sound sources, storage of HRIR data sets, etc. although many of these applications have not been commonly subsumed under the name Ambisonics yet.

Ambisonics has often been regarded being versatile, enabling file exchange, variation in the loudspeaker setups, etc. However, there are many different definitions of channel sequences and normalizations. Moreover, proper reproduction needs the specification of a reference radius, which allows for adaption to playback layouts of different sizes [3, 6, 7]. All this emphasizes the need for a well-defined Ambisonics interchange format that standardizes these parameters. Currently there are some proposals for file formats to be agreed on, c.f. [7, 8, 9, 10].

Establishing an agreed standard is indeed cumbersome for a file format and yet worthwhile, but the standardization of playback layouts should not be a main goal. It is probably the

biggest advantages of Ambisonics that it allows for variation in the actual loudspeaker positions, i.e. angular resampling. But sampling positions cannot be chosen arbitrarily, since they are required to cover an entire circle or sphere as uniformly as possible. However, partial circular/spherical layouts exist [11], and the intention of the present paper is to provide reasonable integration of these into the theoretical framework of Ambisonics, and the format discussion.

The following investigations will show how mode-matching for partial layouts becomes feasible. This is done by harmonics selections based on their symmetry/periodicity properties, likewise by computation of reduced sets of orthogonal base functions for the particular layout. Thereby the latter approach is favorable, since it shows a desirable behavior even outside the considered region, and could be applied to perform angular windowing as well. The reduced number of audio channels is also beneficial for storage and transmission. Merely a simple matrix multiplication is required to restore a default Ambisonics set of signals for playback on full circular/spherical layouts, c.f. Fig. 1. Like proposed in [7], the authors strongly advocate the storage of this reconstruction matrix within a file or streaming format for interchange.

2 AMBISONICS DRIVING FUNCTIONS

Ambisonics uses circular/spherical driving functions, which are represented in terms of harmonics. These harmonics allow for ideally limited angular resolution, i.e. *angular band-limitation*, preceding modal matching with a spatially discrete playback arrangement, cf. [12].

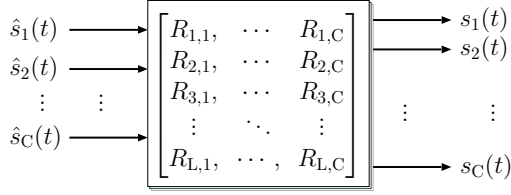


Figure 1: Reconstruction matrix proposed to restore a full set of $L = 2N + 1$ or $L = (N + 1)^2$ ambisonic signals $\{s_l(t)\}_L$ from a smaller set of C transmitted signals $\{\hat{s}_l(t)\}_C$.

1D. An angularly band-limited driving function x for circular Ambisonics playback may be expressed as the Fourier series

$$x(\phi) = \sum_{m=-N}^N \xi_m \Phi_m(\phi), \quad (1)$$

wherein N is the band-limit, ϕ the azimuth angle, ξ_m are real-valued coefficients, and the base functions are *circular harmonics*

$$\Phi_m(\phi) = \sqrt{\frac{2-\delta_m}{2\pi}} \begin{cases} \cos(m\phi) & \text{if } m \geq 0, \\ \sin(m\phi) & \text{if } m < 0. \end{cases} \quad (2)$$

2D. Equivalently, the band-limited driving function x for spherical Ambisonics playback is a Fourier series with dependency on both, the azimuth, and zenith angle (ϕ, θ) , using real-valued coefficients ξ_{nm}

$$x(\phi, \theta) = \sum_{n=0}^N \sum_{m=-n}^n \xi_{nm} Y_n^m(\phi, \theta). \quad (3)$$

In this case, the base functions are *spherical harmonics*

$$Y_n^m(\phi, \theta) = \sqrt{\frac{(2n-1)(n-|m|)!}{2(n+|m|)!}} P_n^{|m|}(\cos \theta) \Phi_m(\phi), \quad (4)$$

composed of associated Legendre functions $P_n^{|m|}$ and circular harmonics.

Note that the driving function x , as well as its coefficients ξ , can be regarded being either a time dependent signal or factors of a mono signal. In Fig. 1, these are represented as Ambisonics signals $\{s_l(t)\}$. This paper uses both interpretations.

Stacked Harmonics Vector Notation. The sums in Eq.(1) and (3) can be re-written as a scalar vector product

$$x = \boldsymbol{\xi}^T \mathbf{b}, \quad (5)$$

with \mathbf{b} being a vector containing the stacked harmonics $\Phi_m(\phi)$ or $Y_n^m(\phi, \theta)$. The coefficients $\boldsymbol{\xi}$ are obtained by the transform integral

$$\boldsymbol{\xi}^T = (x, \mathbf{b}^T)_S. \quad (6)$$

using $(\cdot, \cdot)_S$ to denote integration of a product of functions over the angular domain S (inner product). Whereas for circular harmonics $S = \mathbb{S}^1$ (circle or 1-sphere) and for spherical harmonics $S = \mathbb{S}^2$ (sphere or 2-sphere).

Orthonormality. For band-limited functions x , both *circular/spherical harmonics* form orthonormal and complete sets of functions on either \mathbb{S}^1 or \mathbb{S}^2 . Hence, insertion of Eq. (5) into Eq. (6) yields identity

$$(\mathbf{b}, \mathbf{b}^T)_S = \mathbf{I} \quad (7)$$

3 AMBISONICS ON A BOUNDED CIRCULAR/SPHERICAL DOMAIN

Playback arrangements for Ambisonics frequently do not cover an entire circle or sphere, e.g. a semicircle, hemisphere. Although these arrangements are often chosen due to practical constraints, they might pose non-trivial problems in Ambisonics decoder design by mode-matching.

Decoding problem. This problem is illustrated using a theoretically continuous Ambisonics playback arrangement reproducing the signals $\boldsymbol{\xi}$ on such a fragment, cf. Eq. (5). Re-encoding the playback from this bounded domain $\tilde{S} \subset S$ into Ambisonics signals, cf. Eq. (6), analytically yields a deviation from the original

$$\boldsymbol{\xi}^T \neq \boldsymbol{\xi}^T (\mathbf{b}, \mathbf{b}^T)_{\tilde{S}} = \boldsymbol{\xi}^T \mathbf{G}. \quad (8)$$

The $L \times L$ matrix \mathbf{G} is called Gram matrix. Above it is not the identity matrix, so it indicates that orthonormality of the base-functions \mathbf{b} is lost on \tilde{S} , cp. Eq. (7). This will not be problematic as long as the inverse of \mathbf{G} exists, which can be applied to $\boldsymbol{\xi}^T$ to compensate for the errors $\boldsymbol{\xi}^T = (\boldsymbol{\xi}^T \mathbf{G}^{-1}) \mathbf{G}$. Note that this inversion is usually implicit in Ambisonics decoders computed by mode-matching. Therefore, the existence of an inverse Gram matrix on the continuous domain is regarded a prerequisite to discrete Ambisonics decoding. But frequently the inverse will not exist as linear dependencies emerge, which may render the matrix \mathbf{G} rank deficient

$$\text{rank}(\mathbf{G}) = C < L, \quad (9)$$

i.e. mode-matching fails. Fig. 2 depicts \mathbf{G} for circular harmonics on a semicircular domain $\tilde{S} = [0, \pi]$ up to order $m = 4$. In this example, numerical inversion of \mathbf{G}^{-1} is infeasible as the condition number [13] is too large $\text{cond}(\mathbf{G}) = 3 \cdot 10^5 \gg 1$. In general, the elements of \mathbf{G} can be determined by analytical integration, or estimated using numerical integration [14].

The proposed approach in this paper considers linearly independent base functions other than \mathbf{b} , the Gram matrix of which remains invertible on \tilde{S} .

3.1. Harmonics selection using symmetry/periodicity

Of course, subsets of selected harmonics $\check{\mathbf{b}} \subset \mathbf{b}$ are still orthonormal on the full domain S . Carefully selected harmonics may exhibit common symmetry or periodicity properties, cf. [11]. These harmonics selections even remain orthogonal when integrated over either the symmetric half of their symmetry, or the period of their periodicity. Note that both are bounded domains \check{S} on S , see Fig. 3, hence the following paragraphs deal with these selections $\check{\mathbf{b}}$.

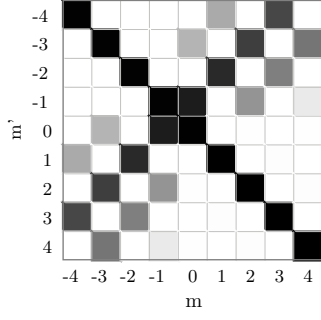


Figure 2: Gram matrix for a semicircular domain.

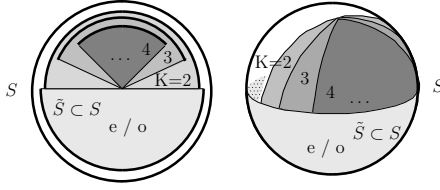


Figure 3: Bounded domains: symmetry halves and periods on the circle and the sphere.

1D symmetries/periodicity. If the driving function $x(\phi)$ is even (or odd) wrt. $\phi = 0$, all sine (respectively cosine) terms must vanish. Moreover, if $x(\phi)$ is a periodic function on a natural fraction of the circle $\frac{360^\circ}{K}$, all ξ_m must vanish, for which m is no integer multiple $k \cdot K$. The circular harmonics exhibit the following symmetry/periodicity properties

$$\Phi_m(\phi) \text{ is } \begin{cases} \text{even,} & \text{for } m \geq 0, \\ \text{odd,} & \text{for } m < 0, \\ \frac{2\pi}{K}\text{-periodic,} & \text{for } m = k \cdot K, k \in \mathbb{Z}. \end{cases} \quad (10)$$

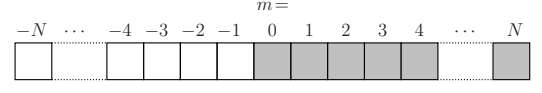
The non-zero coefficients of an even and a π -periodic function are illustrated as colored divisions in Fig. 4(a) and (b).

2D symmetries/periodicity. Obviously, the spherical harmonics have the same azimuthal symmetry/periodicity as the circular harmonics, but also exhibit symmetry properties wrt. $\theta = \frac{\pi}{2}$, which are determined by the associated Legendre functions $P_n^m(\cos \theta)$. They are even/odd functions wrt. $\theta = \frac{\pi}{2}$ depending on whether $m + n$ is even/odd.

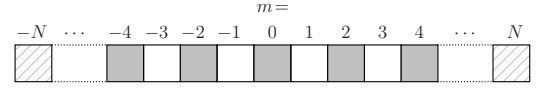
$$Y_n^m(\phi, \theta) \text{ is } \begin{cases} \text{even wrt. } \phi = 0, & \text{for } m \geq 0, \\ \text{odd wrt. } \phi = 0, & \text{for } m < 0, \\ \frac{2\pi}{K}\text{-periodic in } \phi, & \text{for } m = k \cdot K, k \in \mathbb{Z}, \\ \text{even wrt. } \theta = \frac{\pi}{2}, & \text{for } m + n \text{ even,} \\ \text{odd wrt. } \theta = \frac{\pi}{2}, & \text{for } m + n \text{ odd.} \end{cases} \quad (11)$$

In Fig. 4(c) the non-zero coefficients of an even function on the sphere concerning the equator are colored.

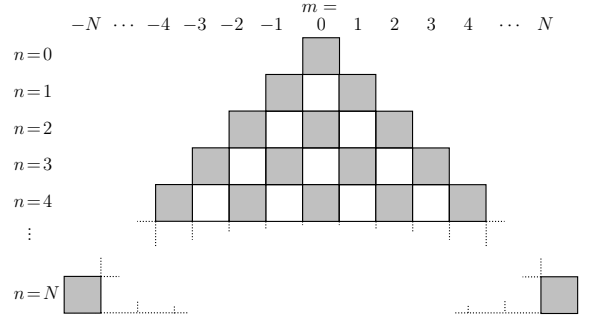
Harmonics selection. Eqs. (10) (11) indicate which harmonics \check{b} to select, to obtain certain symmetry/periodicity properties. We do this by a rectangular matrix \mathbf{R} , containing a single non-zero entry “1” in each row to select match-



(a)



(b)



(c)

Figure 4: Non-zero coefficients (gray divisions) for (a) even functions and (b) π -periodic functions on the circle and (c) functions on the sphere, which are even with respect to the equator.

ing harmonics out of \mathbf{b}

$$\check{\mathbf{b}} = \mathbf{R} \mathbf{b}. \quad (12)$$

A driving function with equal symmetry/periodicity is expressible in $\check{\mathbf{b}}$ by using the coefficients $\check{\xi}^T$

$$x = \check{\xi}^T \check{\mathbf{b}}. \quad (13)$$

To investigate the orthogonality of $\check{\mathbf{b}}$, its Gram matrix can be used. It is easy to show that $(\check{\mathbf{b}}, \check{\mathbf{b}}^T)$ retains its orthonormality $\check{\mathbf{G}} = \alpha \mathbf{I}$ when integrated over the period/symmetric half, up to some scale factor $\alpha = 1/2$ or $1/K$. It relates to the ill-conditioned matrix \mathbf{G} using Eq. (12)

$$\check{\mathbf{G}} = (\check{\mathbf{b}}, \check{\mathbf{b}}^T)_{\check{\xi}} = \mathbf{R} \mathbf{G} \mathbf{R}^T. \quad (14)$$

The conversion of the coefficients is done by left multiplication of Eq. (12) by $\check{\xi}^T$, and comparison with Eq. (5)

$$\check{\xi}^T = \check{\xi}^T \mathbf{R}. \quad (15)$$

A steering vector for the bounded domain can be found by its right inverse $\check{\xi}^T = \check{\xi}^T \mathbf{R}^\dagger$, which is $\check{\xi}^T = \check{\xi}^T \mathbf{R}^T$, here.

Example: Semicircle. For the semicircle $\check{S}=[0, \pi]$, even, odd, and periodic selections are suitable as orthogonal base functions, defined by the matrices

$$\mathbf{R}_e = [\mathbf{0} \quad \mathbf{I}], \quad \mathbf{R}_o = [\mathbf{I} \quad \mathbf{0}], \quad (16)$$

$$\mathbf{R}_p = \begin{bmatrix} \ddots & & & & & \vdots \\ & 1 & 0 & 0 & 0 & 0 & \dots \\ & 0 & 0 & 1 & 0 & 0 & \\ \dots & 0 & 0 & 0 & 0 & 0 & 1 \\ & \vdots & & & & & \ddots \end{bmatrix}. \quad (17)$$

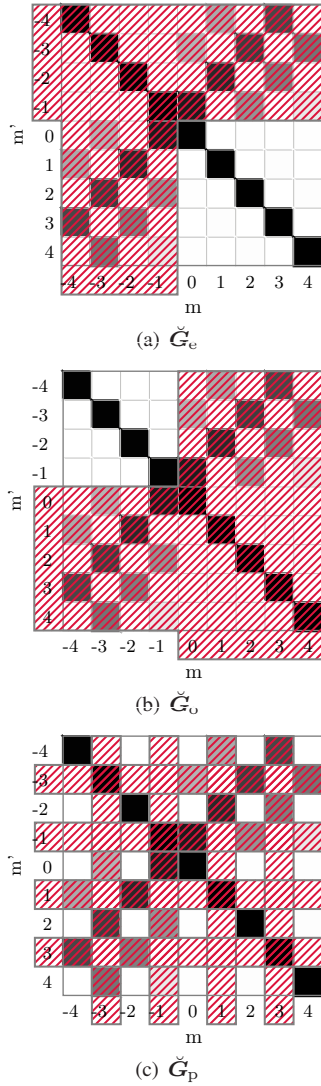


Figure 5: Examples of circular harmonics selection schemes that orthogonalize the Gram-matrix on a semicircular domain: (a) even, (b) odd, or (c) periodic functions.

As depicted in Fig. 5, the Gram-matrices $\check{G} = \mathbf{R}\mathbf{G}\mathbf{R}^T$ of these three selections finally become orthogonal on \check{S} .

Defect 1: Angular limitation. Selecting harmonics $\check{\mathbf{b}}$ with certain symmetry/periodicity works perfectly well for driving functions which are strictly angularly limited to \check{S} . Perfect angular limitation implies unlimited angular resolution, but usually only angularly band-limited driving functions are considered. This leads to unwanted interference due to symmetric/periodic extension of the non angularly limited functions. Fig. 6 illustrates a 1D driving function of a virtual point sources at different angles, using semicircular periodicity and even symmetry. The errors are biggest for sources near the domain boundaries. In particular, periodicity yields a "ghost source" near the opposite boundary, cf. Fig. 6(b), whereas symmetry yields a distorted peak, cf. Fig. 6(c). A further drawback of the harmonics selection approach is that the bounded domain underlies the restrictions of the available symmetry/periodicity axis/planes. Angular

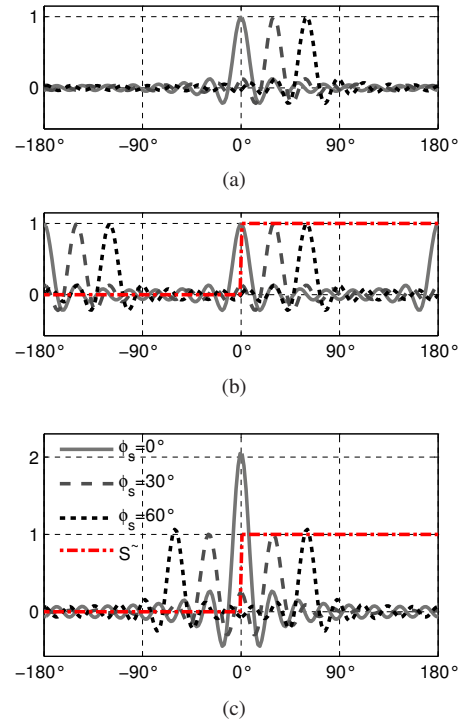


Figure 6: Driving functions of a point source encoded at various angles with (a) a full set of circular harmonics, (b) only π -periodic functions and (c) only the even function (cosine terms).

filtering (max-rE, in-phase, [3]) will cause further degradation, since unwanted source-images spread over the entire domain, also.

Defect 2: Reproduction on full domain. As claimed in the introduction, a versatile format should allow for file interchange, independent of the layout. So a crucial question is, do the selected harmonics allow for sensible reproduction on the full domain? The reduced coefficients vector $\check{\xi}$ can be extended a full set of coefficients ξ by Eq. (15). However, due to the symmetry and periodicity of the selected harmonics, the bounded domain driving function is periodically/symmetrically repeated over the full domain. In general, symmetric or periodic images of the virtual sources are neither acceptable, nor easy to suppress. One possible solution might be angular windowing expressed within the harmonics domain. Appropriate window matrices could be included in \mathbf{R} , but it is infeasible to find low-order window designs achieving satisfactorily steep suppression.

3.2. Other harmonics selection schemes (HVP, FuMa)

There are other selection strategies for the spherical harmonics, cf. [3, 9, 15, 16, 17], which try to enable decoding on irregularly resolved domains. Anisotropic resolution and directional resolution on the sphere are fascinating ideas, but have not been regarded yet for this paper. A closer investigation considering the mathematical evaluation thereof should be considered in future research.

3.3. Band-limited orthonormal base functions for a bounded domain

As mentioned before, arbitrarily shaped bounded domains \tilde{S} do not allow for simple harmonics selections. However, there are other strategies to find base functions that are linearly independent on bounded circular/spherical domains. The approach presented here does not share the elegance of symmetry/periodicity, but circumvents all of its defects; it has been originally outlined in [18].

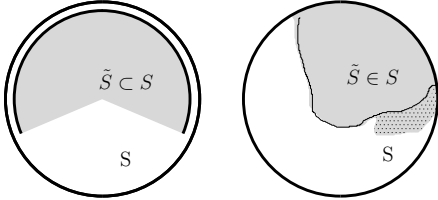


Figure 7: Bounded domains on spheres and circles in general.

New orthonormal band-limited functions. Let's assume a reconstruction matrix \mathbf{R} that computes an angularly band-limited set of base functions $\tilde{\mathbf{b}}$ from \mathbf{b} , which is orthonormal on an arbitrarily bounded domain \tilde{S} , Fig. 7

$$\tilde{\mathbf{b}} = \mathbf{R} \mathbf{b}, \quad (18)$$

$$\tilde{\mathbf{G}} = (\tilde{\mathbf{b}}, \tilde{\mathbf{b}}^T)_{\tilde{S}} = \mathbf{R} \mathbf{G} \mathbf{R}^T = \mathbf{I}. \quad (19)$$

Any band-limited function x defined on \tilde{S} can be expressed as a linear combination of the new base functions

$$x = \tilde{\boldsymbol{\xi}}^T \tilde{\mathbf{b}}, \quad (20)$$

with $\tilde{\boldsymbol{\xi}}$ being a real-valued coefficient-vector.

Orthonormal 1D \rightarrow 2D mapping. If instead of \mathbf{R} the new base functions $\tilde{\mathbf{b}}$ themselves are known, the harmonics \mathbf{b} can be expanded into $\tilde{\mathbf{b}}$ on the bounded domain, yielding the matrix \mathbf{W} , cf. [18]

$$\mathbf{b} = (\tilde{\mathbf{b}}^T, \mathbf{b})_{\tilde{S}} \tilde{\mathbf{b}} = \mathbf{W} \tilde{\mathbf{b}}, \quad (21)$$

which is not always invertible to obtain \mathbf{R} .

In the particular case of cutting out a circular domain from a sphere, e.g. at its equator $\theta = \pi/2$, orthogonal base functions for both, the original and bounded domain, are explicitly given

$$b_{nm} = Y_n^m(\phi, \theta), \quad \tilde{b}_{m'} = \Phi_{m'}(\phi). \quad (22)$$

While disregarding their values on the rest of the sphere, the spherical harmonics evaluated at $\theta = \pi/2$ are exactly expressible in circular harmonics. The elements of this 2D to 1D mapping rule \mathbf{W} are found by the circular harmonics

transform integral of $Y_n^m(\phi, \pi/2)$

$$\begin{aligned} W_{m'}^{nm} &= (\tilde{b}_{m'}, b_{nm}|_{\theta=\frac{\pi}{2}})_{S^1} \\ &= \int_{S^1} Y_n^m(\phi, \frac{\pi}{2}) \Phi_{m'}(\phi) d\phi \\ &= \sqrt{\frac{(2n-1)(n-|m|)!}{2(n+|m|)!}} P_n^{|m|}(0) \int_{S^1} \Phi_{m'}(\phi) \Phi_m(\phi) d\phi \\ &= \sqrt{\frac{(2n-1)(n-|m|)!}{2(n+|m|)!}} P_n^{|m|}(0) \delta_{mm'}. \end{aligned} \quad (23)$$

To achieve conversion from 1D to 2D, a reconstruction matrix is found by the existing pseudo-inverse

$$\mathbf{R} = (\mathbf{W}^T \mathbf{W})^{-1} \mathbf{W}^T. \quad (24)$$

The under-determined system of equations implies that the reconstruction using \mathbf{R} is constrained to be exact at $\theta = \pi/2$, while minimizing the squared magnitude¹ on S^2 . In the literature on beamforming [20], this minimization problem is called minimum-variance distortionless-response (MVDR).

Computation of new base functions by Eigendecomposition. Usually, neither the orthogonal base functions $\tilde{\mathbf{b}}$ on the bounded circular/spherical domain, nor the matrix \mathbf{R} are known. Therefore, the reconstruction matrix \mathbf{R} cannot be computed like in the example above. Nevertheless, a suitable approach can be found in geodesy literature on decomposition restricted spherical domains [18]. This approach finally yields a set of new base functions $\tilde{\mathbf{b}}$ based on the harmonics \mathbf{b} .

Insertion of Eq. (21) into Eq. (8) reveals the relation of \mathbf{W} to the singular Gram-matrix \mathbf{G} of \mathbf{b}

$$\mathbf{G} = (\mathbf{b}, \mathbf{b}^T)_{\tilde{S}} = \mathbf{W} (\tilde{\mathbf{b}}, \tilde{\mathbf{b}}^T)_{\tilde{S}} \mathbf{W}^T = \mathbf{W} \mathbf{W}^T, \quad (25)$$

which can be computed by numerical/analytical integration. Due to its structure, \mathbf{G} can be factorized using real-valued eigendecomposition

$$\mathbf{G} = \mathbf{W} \mathbf{W}^T = \mathbf{V} \mathbf{D} \mathbf{V}^T, \quad (26)$$

hereby \mathbf{D} is a diagonal matrix containing the eigenvalues and \mathbf{V} is a square matrix, the columns of which are the corresponding eigenvectors.

Reconstruction matrix by regularization. From Eqs. (25) (19) we see that \mathbf{R} should be left inverse to \mathbf{W}

$$\tilde{\mathbf{G}} = \mathbf{R} \mathbf{W} \mathbf{W}^T \mathbf{R}^T \stackrel{!}{=} \mathbf{I}, \quad (27)$$

but since \mathbf{G} becomes rank-deficient, i.e. some eigenvalues will be close to zero, and \mathbf{R} will not exist

$$\mathbf{R} = \text{diag}\{1/d_1, 1/d_2, \dots, 1/d_C, \underbrace{1/0, \dots, 1/0}_{\#}\}^{1/2} \mathbf{V}^T. \quad (28)$$

¹Note that this minimization will only work using the fully normalized spherical harmonics due to the Parseval theorem, cf. [19]. Semi-normalized spherical harmonics will lead to weak minimization of the higher order harmonics and therefore are suboptimal.

However, using the eigenvectors V_C associated with the non-zero eigenvalues $D_C = \text{diag}\{d_1, d_2, \dots, d_C\}$ exclusively, yields a smaller set of orthonormal functions, for which orthonormality holds

$$D_C^{-1/2} V_C^T V_C D_C V_C^T V_C D_C^{-1/2} = I_C. \quad (29)$$

These new base functions are

$$\tilde{\mathbf{b}} = \mathbf{R} \mathbf{b}, \quad \mathbf{R} = D_C^{-1/2} V_C^T. \quad (30)$$

Essentially, this already is the final result, but the angular harmonics \mathbf{b} will usually appear strongly mixed in the new base functions $\tilde{\mathbf{b}}$. Therefore, $\tilde{\mathbf{b}}$ will lose any evident relation to angular resolution or wave-length.

De-mixed base functions by triangular decomposition (QR).

As given in [18], a more de-mixed set of base functions can be determined by QR -decomposition of the reconstruction matrix \mathbf{R} into an orthonormal matrix \mathbf{Q} and an upper triangular matrix $\hat{\mathbf{R}}$

$$\tilde{\mathbf{b}} = \mathbf{R} \mathbf{b} = \mathbf{Q} \hat{\mathbf{R}} \mathbf{b}. \quad (31)$$

The orthonormality is exploited by left-multiplying Eq.(31) with \mathbf{Q}^T , and yields the base functions $\hat{\mathbf{b}} = \mathbf{Q}^T \tilde{\mathbf{b}}$

$$\hat{\mathbf{b}} = \hat{\mathbf{R}} \mathbf{b}. \quad (32)$$

Due to the triangular structure of $\hat{\mathbf{R}}$, the angular harmonics appear less mixed in $\hat{\mathbf{b}}$ than in $\tilde{\mathbf{b}}$, so an interpretation in terms of angular wave-lengths becomes easier. Note that the particular result depends on the sequence of the harmonics in \mathbf{b} : The functions at the bottom of $\hat{\mathbf{b}}$ contain the smallest number of mixed harmonics, which will be combinations of the harmonics at the bottom of \mathbf{b} , in particular.

Reconstruction matrix, steering vector. Comparison after left multiplication of Eq. (32) by the expansion coefficients $\hat{\xi}^T$ yields the conversion rule for coefficients, with the reconstruction matrix $\hat{\mathbf{R}}$

$$\xi^T = \hat{\xi}^T \hat{\mathbf{R}}. \quad (33)$$

Its pseudo-inverse $\hat{\mathbf{W}} = \hat{\mathbf{R}}^\dagger = V_C D_C^{1/2} \mathbf{Q}$ is helpful as well, if a given Ambisonics signal shall be bounded to the domain \tilde{S} by conversion into $\hat{\xi}$, or a steering vector shall be found from its harmonics equivalent ξ on the full domain.

Decoding. Given the $Q \times L$ matrix \mathbf{B} with the harmonics suitably sampled at Q discrete loudspeakers locations on a bounded circular/spherical domain, a decoder is defined by the mode-matching equation

$$\xi^T \stackrel{!}{=} \mathbf{g}^T \mathbf{B}, \quad (34)$$

wherein \mathbf{g} are the driving weights for the loudspeakers. Usually, right inversion of \mathbf{B} fails, but $\hat{\mathbf{B}} = \mathbf{B} \hat{\mathbf{W}}$ is invertible:

$$\begin{aligned} \hat{\xi}^T &\stackrel{!}{=} \mathbf{g}^T \hat{\mathbf{B}}, \\ \Rightarrow \mathbf{g}^T &= \hat{\xi}^T \hat{\mathbf{B}}^T (\hat{\mathbf{B}}^T \hat{\mathbf{B}})^{-1}. \end{aligned} \quad (35)$$

Example: 3/10 portion of a circle. The example given in Fig. 8 shows the performance of the proposed approach. The illustrations depict a virtual point source near the border of a bounded circular domain, using 3/10 of a circle and a cut-off order of $N = 15$. From the original 31 base functions, a reduction to 12 functions was found sufficiently regular and accurate. Astonishingly, this approach yields reasonable rejection outside of \tilde{S} , in contrast to symmetry/periodicity based harmonics selections. The actual base functions are plotted in Fig. 9. For the triangular decomposition, the harmonics have been sorted so that the first base-functions contain lower-order harmonics, mainly.

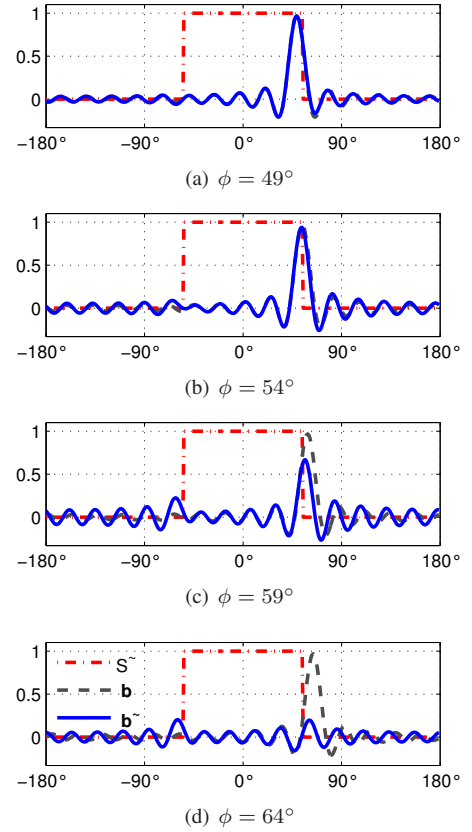


Figure 8: Driving functions of a point source on 3/10 of a circle $\tilde{S} = [-54^\circ, 54^\circ]$, using the 12 base functions $\hat{\mathbf{b}}$ depicted in Fig. 9 compared the full set of 31 circular harmonics \mathbf{b} encoded at various angles near the domain boundary, $N = 15$.

4 FILE FORMAT

From discussions at the institution of the authors, several ideas on the design of a suitable Ambisonics exchange format have been found, which will be summarized here. Fig. 10 illustrates information items that are considered important.

File contents: An Ambisonics file format is probably the best container for spherically irradiating, as well as spherically radiating sound fields. Therefore, a suitable file format

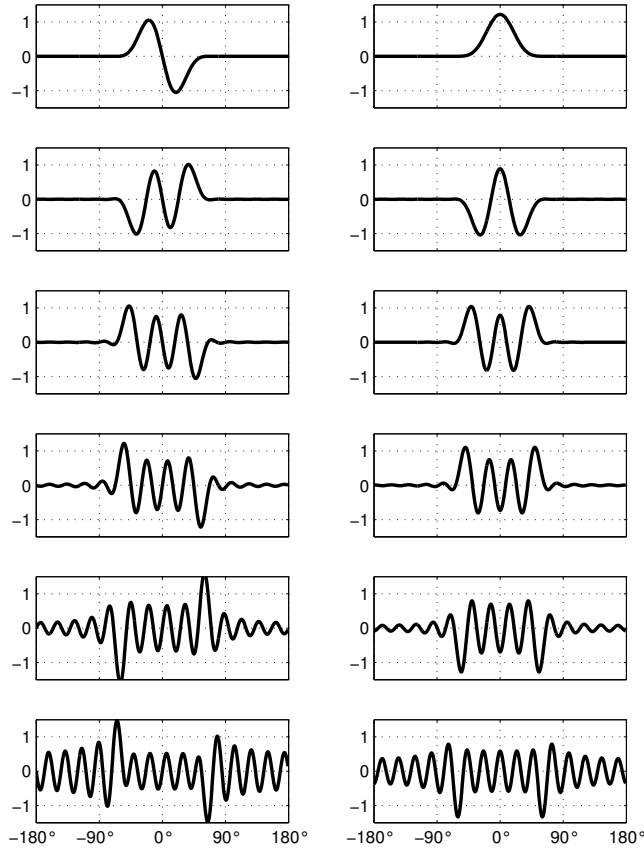


Figure 9: 12 base functions \hat{b} on $3/10$ of a circle $\tilde{S} = [-54^\circ, 54^\circ]$ using $N = 15$.

should be capable of containing

1. incident sound fields recorded with compact circular/spherical microphone arrays
2. studio/art productions rendered for circular or spherical (binaural) Ambisonics playback *with or without distance coding, enabling reconstruction from bounded circular/spherical domain signals*
3. (individual) spherical harmonics head related impulse responses *facilitating binaural Ambisonics rendering and angular resampling/interpolation*
4. sound radiation of sources recorded with big circular/spherical microphone arrays *for playback with compact spherical loudspeaker arrays, or auralization/rendering using object (source) oriented spatial rendering*
5. studio/art productions rendered for compact spherical loudspeaker arrays

Some of the above data are also important for object related mixing approaches [21], as they provide source directivity information, but also allow for inclusion of Ambisonics playback from recordings/productions. Conversely, as the object related mixing approach is also flexible with respect to different spatial audio rendering techniques, Ambisonics

can be used as an output format [22, 23].

Required Data: For distance-coding, the *reference radius* is a necessary information that describes for which size the Ambisonics production has been rendered [7, 24, 12]. But also for source radiation recordings, spherical harmonics HRIRs, spherical microphone array recordings, as well as productions for compact spherical loudspeaker arrays, the specification of a *reference radius* is mandatory. If given in meters, the speed of sound also needs to be specified. Alternatively, the reference radius can be specified as a flight-time in samples.

The promising examples show that Ambisonics can be extended to describe driving functions for fragments (arcs, segments, belts, ...) of circular/spherical layouts. The required set of signals is reduced to a smaller set. Ambisonics playback from these signals is obtained by a reconstruction matrix. Reconstruction is always feasible without severe degradation, as good suppression on the unused angular portion is achievable. The *reconstruction matrix* is considered as mandatory to enable interchange of partial circular/spherical domain material.

Furthermore, the extension of the file by further metadata could be quite useful.

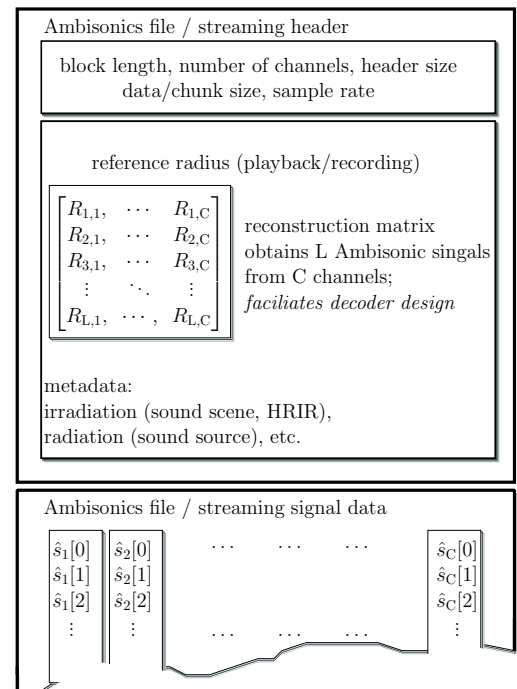


Figure 10: Proposed contents of an Ambisonics file/streaming format.

5 CONCLUSION

This paper has successively presented a symmetry/periodicity based approach, and an outperforming eigendecomposition-based approach. The latter extends Ambisonics decoding so that it also works on bounded

circular/spherical playback arrangements. Therefore, loudspeaker layouts can be made more flexible. Furthermore, this technique has the effect of angular windowing (without using convolution/Gaunt-coefficients explicitly). It turns out that Ambisonics uses a reduced set of base functions on the partial circles/spheres, which allows for a reduced effort in audio-transmission or storage. To make this reduction accessible, while remaining compatible to full default Ambisonics sets, a reconstruction matrix has to be used in the file/audio stream. One of the shortcomings of this approach is that distance coding will only work with restrictions. Anisotropic, or directional resolution approaches have not been tested within this work and might be subject to future studies.

6 ACKNOWLEDGMENTS

The authors thank the IEM Ambisonics discussion group (Alois Sontacchi, Thomas Musil, Johannes Zmöllnig, Winfried Ritsch) and its guests for many discussions on reconstruction matrices, file format requirements, weaknesses and strengths, as well as the position of Ambisonics in the discussion spatial audio and its description. Furthermore, the authors gratefully thank the Austrian Research Promotion Agency (FFG), the Styrian government and the Styrian business promotion agency (SFG) under the COMET program for their support.

REFERENCES

- [1] M. A. Gerzon, "Periophony (with-height sound reproduction)," in *Proc. of the AES 2CE Conv., Munich*, March 1972.
- [2] J. Bamford and J. Vanderkooy, "Ambisonic sound for us," in *Proc. of the 99th AES Conv., New York*, October 1995.
- [3] J. Daniel, "Représentation de champs acoustiques, application à la transmission et à la reproduction de scènes sonores complexes dans un contexte multimédia," Ph.D. dissertation, Université Pierre et Marie Curie (Paris VI): Paris, 2001.
- [4] S. Moreau, "Étude et réalisation d'outils avancés d'encodage spatial pour la technique de spatialisation sonore Higher Order Ambisonics: microphone 3D et contrôle de distance," Ph.D. dissertation, Université du Maine, 2006.
- [5] Z. Li, "The capture and recreation of 3D auditory scenes," Ph.D. dissertation, University of Maryland, College Park, 2005.
- [6] A. Laborie, R. Bruno, and S. Montoya, "Reproducing multichannel sound on any speaker layout," in *Proc. of the 118th AES Conv., Barcelona*, 2005.
- [7] ISO/IEC 14496-11:2003 *Information technology - Coding of audio-visual objects - Part 11: Scene description and application engine, Adment 3: Audio BIFS Extensions*; (Jerome Daniel), Std., 2003.
- [8] M. Chapman, W. Ritsch, T. Musil, I. Zmöllnig, H. Pomberger, F. Zotter, and A. Sontacchi, "A Standard for Interchange for Ambisonics Signal Sets - Including a file standard with metadata," in *Proc. of the Ambisonics Symposium, Graz*, June 2009.
- [9] Ambisonics. [Online]. Available: <http://groups.google.com/group/ambisonics>
- [10] Ambisonics-xchange. [Online]. Available: <http://ambisonics.iem.at/>
- [11] A. Sontacchi, F. Zotter, and R. Höldrich, "3d sound field rendering under non-idealized loudspeaker arrangements," in *Proc. Acoustics-08, Paris*, 2008.
- [12] F. Zotter, H. Pomberger, and M. Frank, "An Alternative Ambisonics Formulation: Modal Source Strength Matching and the Effect of Spatial Aliasing," in *Proc. of the 126th AES Conv., Munich*, May 2009.
- [13] Condition number. [Online]. Available: http://en.wikipedia.org/wiki/Condition_number
- [14] N. Sneeuw, "Global spherical harmonic analysis by least-squares and numerical quadrature methods in historical perspective," *Geophys. J. Int*, vol. 118, no. 3, pp. 707–716, 1994.
- [15] C. Travis, "A new mixed-order scheme for ambisonic signals," in *Proc. of the Ambisonics Symposium, Graz*, June 2009.
- [16] Ambisonics. [Online]. Available: <http://en.wikipedia.org/wiki/Ambisonics>
- [17] M. Chapman. Ambisonic channels. [Online]. Available: <http://ambisonics.ch/standards/filetypes/>
- [18] R. Pail, G. Plank, and W. Schuh, "Spatially restricted data distributions on the sphere: the method of orthonormalized functions and applications," *Journal of Geodesy*, vol. 75, no. 1, pp. 44–56, 2001.
- [19] E. Williams, *Fourier Acoustics: sound radiation and nearfield acoustical holography*. Elsevier, 1999.
- [20] D. Ward and M. Brandstein, *Microphone Arrays: Signal Processing Techniques and Applications*. Springer, 2001.
- [21] G. Gatzsche and F. Melchior, "Spatial Audio Authoring and Rendering: Forward Research Through Exchange," in *Proc. of the ICMC, Belfast*, August 2008.
- [22] F. Zotter, "Mehrkanalaustauschformat für 3D Audio Ambisonics," in *5. Thüringer Medienseminar, Erfurt*, 2009. [Online]. Available: http://iem.at/Members/zotter/zotter_5thms.zip
- [23] F. Melchior, A. Gräfe, and A. Partzsch, "Spatial Audio Authoring for Ambisonics Reproduction," in *Proc. of the Ambisonics Symposium*, 2009.
- [24] J. Daniel, "Spatial sound encoding including near field effect: Introducing distance coding filters and a viable, new ambisonics format," in *Proc. AES 23rd Conference, Copenhagen*, 2003.